Mapping of variables in FE analysis of arbitrary cohesive crack propagation

R. A. Einsfeld
Polytechnic Institute (IPRJ), State University of Rio de Janeiro (UERJ), Nova Friburgo, RJ – Brazil

Abstract

The cohesive crack is the simplest model that describes the fracture process in concrete structures. In such model, the fracture process zone can be described either by the discrete or by the smeared approaches. In the simplest formulation of cohesive crack model using the discrete approach, all the body volume remains elastic, and the nonlinearity is included in the boundary conditions along the crack line. When the crack path is known *a priori*, the analysis through this approach is easy to implement and available in most commercial FEM codes. If the crack path is not known in advance, the use of remeshing techniques is necessary in order to simulate the crack growth. When plasticity models are used for the concrete, special schemes are required to map the solution variables from the old to the new finite element model in order to proceed with the analysis. Apparently, this is a major drawback for the development of a general FEM code for arbitrary cohesive crack propagation using the discrete approach. In this paper, it is presented a technique for mapping the solution variables when an energy-based plasticity model for concrete is used, and the discrete crack growth continuously modifies the mesh topology during the analysis. An example is presented to show the improvements obtained using this technique.

Keywords: fracture mechanics of concrete, cohesive crack models, plasticity, mapping of variables

1 Introduction

The fracture process in concrete is characterized by a large region ahead of the crack tip where the micro-cracks develop until they coalesce into a macro-fracture. This region, which has a longitudinal characteristic shape, is called fracture process zone. The recognition of this characteristic, and the application of the concepts developed by Hillerborg, Modéer and Petersson [1] for the nonlinear fracture mechanics of concrete, enabled the development of several numerical models for simulation of plain and reinforced concrete structures behavior.

The fracture process zone can be described either by the discrete crack approach, where the entire fracture process zone is lumped into the crack line and is characterized in the form of a stress-displacement law which exhibits softening, or by the smeared crack approach, where the inelastic

Mechanics of Solids in Brazil 2007, Marcílio Alves & H.S. da Costa Mattos (Editors)
Brazilian Society of Mechanical Sciences and Engineering, ISBN 978-85-85769-30-7

deformations in the fracture process zone are smeared over a band of a certain width, imagined to exist in front of the main crack [2].

The smeared crack approach offers a number of advantages over the discrete approach. Remeshing techniques and continuous topological redefinition are not necessary in the smeared process. Also, the rotation of principal stress axes can be treated during the strain softening. The major disadvantage of the smeared process, however, is its inability to model the surfaces of the crack. In consequence, the representation of cracked material as a continuum induces locked-in stress in the elements close to the localization zone [3] and a response of the structure that is too stiff is frequently found in the analysis.

To simulate discrete crack propagation, many commercial FEM codes have nonlinear spring elements with user-defined stress strain curves that can be easily used when the crack path is known *a priori*. If the crack path is not known in advance, remeshing techniques are required for this kind of approach.

Automatic remeshing techniques for FEM analysis have been implemented in a few codes. The basic technology has improved along with computer graphics capabilities and the development of sophisticated data structures, which assures the mesh consistency. Nevertheless, these techniques have been applied mostly to linear elastic problems. In this case, mapping the local variables from the old mesh to the new one, after discrete crack insertion or propagation, is straightforward. With the increasing use of non-linear FEM analysis applied to inelastic problems, the mapping of local variables from the old to the new finite element model has become a major issue of interest due to its influence on the sequence of the numerical analysis.

In the following section, some techniques for simulation of arbitrary discrete crack propagation are described. The mapping techniques for transferring the solution variables after remeshing due to crack insertion and propagation are described in section 3. In section 4, an example is presented to show the improvements obtained using the technique implemented by the author.

2 Discrete representation of arbitrary crack growth

The discrete propagation using the linear elastic fracture mechanics (LEFM) theory was studied by Ingraffea and co-workers at Cornell University. The FRANC2D system [4] was developed for simulation of arbitrary cracks growth with automatic remeshing in two-dimensional, linear elastic finite element models. Such a system produces a numerical stress intensity vs. crack length relationship which can be used in conjunction with a crack growth rate model to predict crack length and stability over time [5]. Quarter-point singular elements, forming a rosette pattern, are used to capture the stress-strain singularity at the crack tip. Therefore, an initial crack has to be assumed in order to position the rosette into the original mesh. The stress intensity factors are then computed from results of the analysis using a specified calculation technique. Further details on this process can be found in references [6] and [7]. Starting from an initial crack, such a procedure can be useful to analyze crack trajectory in mass concrete structures as gravity dams.

To simulate arbitrary cohesive crack propagation using the FRANC system, a special algorithm was proposed by Bittencourt et al. [8]. In this strategy, linear elastic quadrilateral and triangular elements are used in conjunction with zero-thickness interface elements in the fictitious crack. The criterion for

Mechanics of Solids in Brazil 2007, Marcílio Alves & H.S. da Costa Mattos (Editors)
Brazilian Society of Mechanical Sciences and Engineering, ISBN 978-85-85769-30-7

propagation is based on the fictitious crack tip opening profile. Although the rosette pattern is still present at the crack tip, no singular elements are used to form it. Here again, an initial crack has to be assumed in order to start the analysis.

A hybrid formulation to simulate arbitrary cohesive crack propagation, which considers the discrete and smeared approaches, was implemented and tested with relative success by the author [9]. In this method, there is no need to assume an initial crack to start the analysis. The smeared process, with an energy-based plasticity model for concrete, is used to predict the strain localization and the corresponding discrete crack position and direction. Due to discrete crack insertion or propagation, the geometry of the model is modified and the region around the crack is remeshed. Then, nodal displacements and history-dependent variables are mapped from the old mesh configuration to the new one. The use of triangular elements gives more flexibility in creating new acceptable meshes in irregular domains. The process is illustrated in Figure 1 according to the following sequence: a) identification of the element (integration point) where the material softening behavior occurs; b) elimination of the identified element and all the surrounding elements; c) insertion of the discrete crack; d) remeshing of the region around the crack.

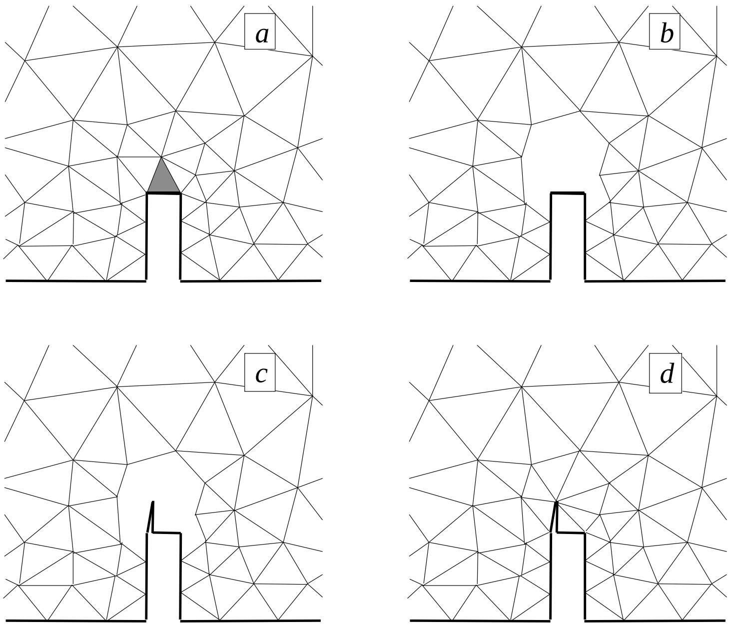

Figure 1: Procedure for discrete crack insertion [9].

The criterion to discrete crack insertion is based on the energy dissipation on the integration points where the material softening behavior occurs. The concrete softening behavior is characterized by the tensile strength $f_t^{'}$ and the fracture energy G_F, which is a material parameter determined experimentally as described in reference [10]. The numerical procedure accounts for the evidence that the representation of the cracked material as a continuum induces locked-in stress in the elements close to the localization zone [3]. Due to finite element nodes compatibility, the smeared process induces the plastic behavior over a relatively large region and causes difficulties for the occurrence of strain localization in a single element. Therefore, the discrete crack is inserted or propagated when the softening stress at the identified integration point shows a minimum variation between two consecutive steps, evidencing that the plastic behavior had already been induced for the neighboring elements at this stage of the analysis. This problem was partially alleviated by using triangular elements, allowing mesh lines with different inclinations, some aligned with the crack path.

The crack length is evaluated based on the characteristic length of the corresponding element [3] and the crack direction follows the criterion of Erdogan and Sih [11]. This criterion states that the crack path is perpendicular to the maximum principal stress. All topological modifications due to crack propagation are managed by an underlying half-edge data structure [12], which assures the mesh consistency. The remeshing algorithm accounts for a quadtree procedure and a boundary-contraction scheme as described in references [6] and [7].

The indirect displacement control was used in order to improve numerical convergence. Once the discrete crack was inserted, the numerical convergence process became controlled by the degrees-of-freedom that correspond to the crack opening nodes. In spite of the various numerical strategies applied to solve the system of equations, the representation of crack propagation was only possible up to a certain degree, after what it was not possible to proceed with the analysis because numerical convergence was no longer obtained. It was later verified that unbalanced forces, occurring in nodes released after the discrete crack insertion, could undermine the numerical convergence. The use of interface elements was proposed in order to control these forces [13], but this procedure is still not implemented to date in the numerical model. However, in the course of the hybrid formulation implementation, it became apparent that the numerical instability could also be attributed to the strategy used for mapping the solution variables. With the use of energy-based plasticity model for concrete, special mapping schemes are required, as shown in the next section.

3 Mapping of solution variables

The problem of mapping solution variables in elastoplastic problems was treated by Lee and Bathe [14] when using a system of adaptive procedures for large-deformation finite element analysis. Because of large deformation, an element or a group of elements can become distorted and consequently undermine the numerical analysis. Therefore, at a certain stage of the analysis, a new finite element model must be constructed over the distorted mesh in order to avoid the large deformation effects.

Mapping strategies are also necessary in elastoplastic FEM analysis of arbitrary discrete crack propagation with remeshing. It is necessary to transfer the solution variables from the old to the new finite element model to enable the analysis to proceed from the current time step using the new model. The solution variables consist of the nodal displacements and the history-dependent variables.

Mechanics of Solids in Brazil 2007, Marcílio Alves & H.S. da Costa Mattos (Editors)
Brazilian Society of Mechanical Sciences and Engineering, ISBN 978-85-85769-30-7

3.1 Mapping of nodal displacements

Using the same notation as Lee and Bathe [14], the mapping of nodal displacements can be stated as:

$$ {}^{t}u_o({}^{t}V) \rightarrow {}^{t}u_N({}^{t}V) \tag{1} $$

where ${}^{t}u_o$ is the displacement field given by the old finite element model at time t, and ${}^{t}u_N$is the displacement field given by the new finite element model at time t. Both finite element models cover the same domain V at time t.

The mapping process is exemplified in Figure 2. For each node n of the new mesh, the element of the old mesh where node n lies is located. The displacements at this new node are then obtained using the shape functions corresponding to this element:

$$ {}^{t}u_N^n = \sum_{k=1}^{K_0} h_k(r_o^n, s_o^n)\,{}^{t}u_o^k \tag{2} $$

where k is the current node number in the old element, K_0 is the total number of nodes of the old element, h_k are the shape functions related to the old element, and r_o^n and s_o^n are the parametric coordinates of node n in relation to the old element. For the quadratic triangular elements used in this work, a good approximation for the parametric coordinates is obtained computing the area coordinates considering the undistorted element.

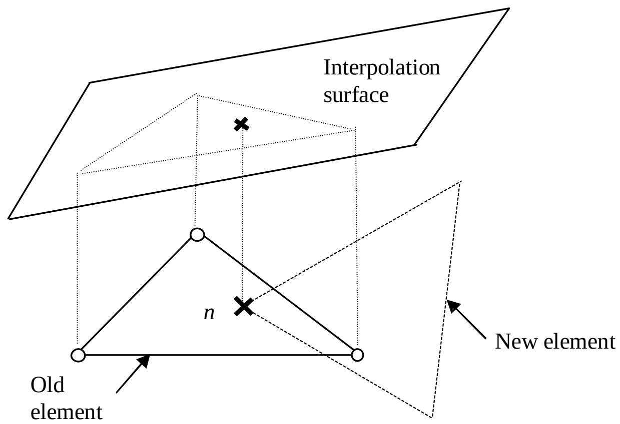

Figure 2: Mapping of node displacements from the old model to node n of the new mesh [15].

3.2 Mapping of history-dependent variables

The mapping process for the history-dependent variables can be stated as:

$$^{t}l_o(^{t}V) \rightarrow {}^{t}l_N(^{t}V) \tag{3}$$

where $^{t}l_o$ and $^{t}l_N$ are the list of history-dependent variables of the old and new FE models, respectively.

The history-dependent variables consist of the stresses, the plastic deformation increment, the equivalent plastic strain and the current yield strain. A number of schemes to accomplish this task were tested and they resulted in a better representation of the fracturing process. The implemented strategies consider the use of quadratic triangular elements in the analysis.

In the first strategy tested, all the variables were mapped at time t from the old mesh to the new Gauss (integration) point by using a least square fit over the integration points of the old element. For each Gauss point g in the new mesh, the element of the old mesh where point g lies is located, and the mapping process for the stresses can be stated as:

$$^{t}\sigma_N{}^{g} = \sum_{k=1}^{3} h_k^{'}(r_o^g, s_o^g)^{t}\sigma_o{}^{k} \tag{4}$$

where $^{t}\sigma_N^g$ is the new stress at time t, $^{t}\sigma_o^k$ is the old stress relatively to each old Gauss point k, $h_k^{'}$ are the linear shape functions related to the old mesh and r_o^g and s_o^g are the parametric coordinates of node g in relation to the old element. The process is illustrated in Figure 3.

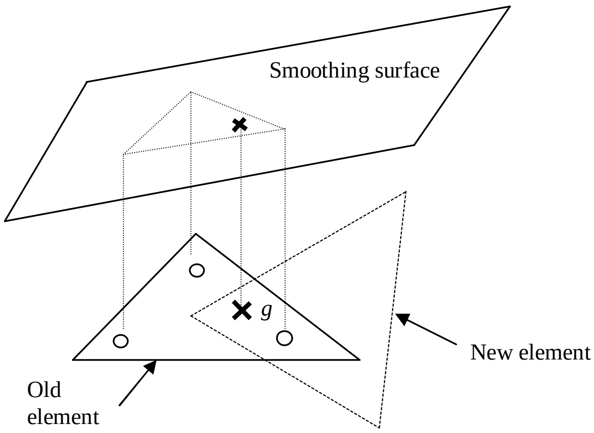

Figure 3: Mapping of history-dependent variables from the old mesh to new integration point [15].

As can be observed from Figure 3, it is possible to obtain interpolated or extrapolated values for the stresses. In some situations the process has to take into account the limit yield stress and relax the extrapolated stress on the limit loading surface. The results obtained for the equivalent plastic strain, compared with the maximum equivalent pre-peak strain, determine the material pre-peak or post-peak behavior at Gauss point g.

The main drawback of this approach, however, is that it does not assure consistency between stresses and strains, and unexpected elastic unloading occurred at some integration points. Therefore, new schemes driven to assure stress-strain consistency were tested using an auxiliary triangular Gauss point mesh associated to the old finite element mesh, as shown in Figure 4. It was introduced in the methodology to avoid situations where the approximations obtained for the stresses correspond to extrapolated values. For each Gauss point g in the new mesh, the triangle in the auxiliary mesh where point g lies is identified. The new values for the stresses are then mapped using linear interpolation functions related to the nodes of the triangle.

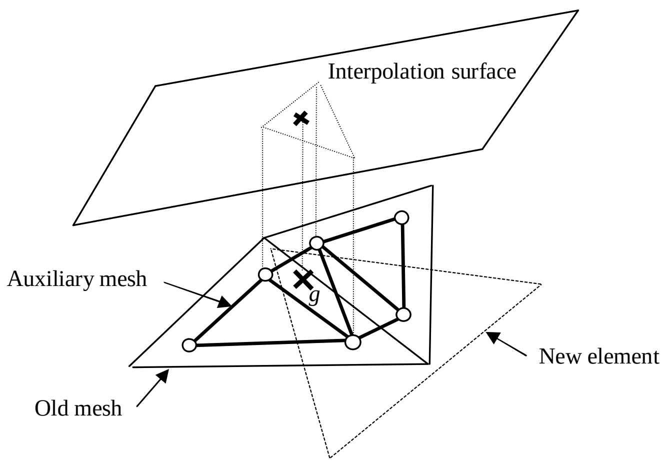

Figure 4: Application of an auxiliary triangular Gauss point mesh.

In this new strategy, the history-dependent variables are mapped from the old mesh to the new mesh at time t-Δt, and then transferred to the new model at time t using the trial elastic strain increment. This procedure assures that the consistency of the solution variables is satisfied at time t. The trial elastic strain increment is obtained from the displacements mapped from the old to the new model at time t, using the same methodology applied in the first strategy.

The aforementioned approaches were presented in a previous work by Einsfeld et al. [15]. As an improvement of the schemes tested before, a new procedure for mapping solution variables was implemented. The main difference in relation to the previous scheme is that the stresses are no longer mapped from the old to the new model at time t-Δt. Instead, they are obtained from the trial elastic strain according to the following steps:

1. Mapping of material constitutive parameters *(mcp)* at time t-Δt, obtaining ${}^{t-\Delta t}$*(mcp)*;
2. Mapping of total strain and plastic strain at time t-Δt, obtaining, respectively, ${}^{t-\Delta t}\varepsilon_{total}$ and ${}^{t-\Delta t}\varepsilon^{p}$;
3. Mapping of the displacements at time t, obtaining ${}^{t}\boldsymbol{u}$;

4. Obtain the total strain at time t: ${}^t\varepsilon_{total} = {}^t\boldsymbol{B}{}^t\boldsymbol{u}$, where $\boldsymbol{B}$ is the strain-displacement matrix;
5. Compute the trial elastic strain: ${}^t\varepsilon^{*e} = {}^t\varepsilon_{total} - {}^{t-\Delta t}\varepsilon^p$;
6. Compute the trial elastic stress: ${}^t\sigma^* = \boldsymbol{D}{}^t\varepsilon^{*e}$, where $\boldsymbol{D}$ is the elasticity matrix;
7. Obtain the strain increment (supposed elastic): ${}^t\Delta\varepsilon = {}^t\varepsilon_{total} - {}^{t-\Delta t}\varepsilon_{total}$,
8. Obtain the stresses at time t-Δt: ${}^{t-\Delta t}\sigma = {}^t\sigma^*$ - $\boldsymbol{D}{}^t\Delta\varepsilon$;
9. Enter in the constitutive driver with: ${}^{t-\Delta t}\sigma$, ${}^{t-\Delta t}$*(mcp)*, ${}^t\Delta\varepsilon$;
10. Obtain at time t: ${}^t\sigma$, ^{t} *(mcp)*, and ${}^{t-\Delta t}\varepsilon^p$.

The results obtained for discrete crack growth simulation using this last approach are presented in the next section.

4 Example of arbitrary crack growth simulation

A 2D numerical model, considering the hybrid formulation proposed by the author [9], has been implemented in order to investigate arbitrary discrete crack growth in concrete structures. The model is comprised by a set of integrated finite element and interactive computer graphics routines. The interactive computer graphics plays an essential role in discrete crack analysis. It allows the generation of the initial structural model, automatic remeshing after discrete crack insertion and visualization of the results obtained by the numerical analysis. The pre-processor MTOOL [16] has been used for pre-processing and has been adapted for remeshing tasks. The pre-processor is supported by the half-edge data structure [12] that assures mesh consistency. For FEM analysis, the program FEPARCS, developed by Elwi [17] has been adapted for the tasks of remeshing and mapping of the solution variables. The concrete behavior was simulated through the energy-based plasticity model of Pramono and Willam [18].

A numerical simulation was carried out for mixed-mode fracture specimen. The objective of this example is to show the capacity of the model to simulate curvilinear crack trajectories. Figure 5 shows the finite element mesh idealization. The supports and the loading conditions are non-symmetric with respect to the notch. The mesh was arbitrarily generated using quadratic isoparametric triangular elements (T6). The dimensions of the beam are 1322x306 mm^2 (length x height) with a notch of 10x82 mm^2 (width x depth), as in the work of Arrea and Ingraffea [19]. The material parameters are: tensile strength $f_t^{'} = 2.8$ MPa, fracture energy with exponential softening diagram $G_F = 55$ N/m, modulus of elasticity $E = 30000$ MPa and Poisson's ratio $v = 0.18$.

The model was tested using the mapping schemes presented in the previous section. When the solution variables are mapped by simple interpolation at time t, corresponding to the first strategy presented, the numerical convergence was no longer achieved after the first step of crack propagation. Using the last mapping scheme presented, with the interpolation of the history-dependent variables performed through the auxiliary Gauss point mesh, the numerical convergence improved relatively to the previous scheme, allowing more steps of crack propagation. The deformed configuration of the beam is shown in Figure 6.

A comparison between observed and predicted crack trajectories is presented in Figure 7. The crack starts with an initial inclination of 45° in the right corner of the notch and surpass the loading line as shown in the figure. According to Rots [3], this curvilinear crack trajectory, observed in the

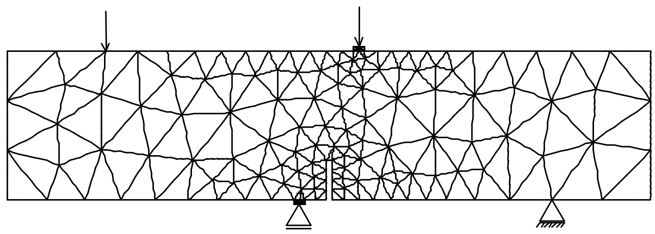

Figure 5: Finite element mesh for notched beam in mixed-mode fracture.

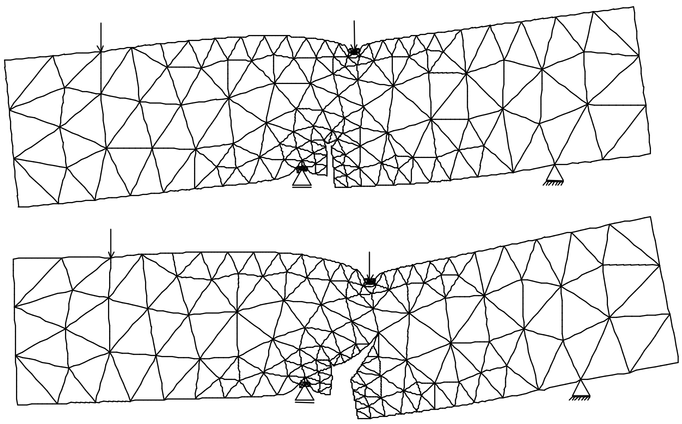

Figure 6: Deformed configuration (x500): shear mode *(above)* and opening mode *(below)*.

experiments, can only be reproduced by the discrete crack approach.

5 Concluding remarks

In this work, some schemes for mapping solution variables due to remeshing are presented. These schemes are applied to discrete representation of cohesive crack growth in concrete structures. In performing the numerical experiments, it was verified that the sequence of the analysis depends strongly on the approximations obtained for these variables. When the first strategy was adopted, one would think that the approximations obtained mapping all the variables at time t would be sufficient to restore the stress-strain field configuration and would allow the sequence of the analysis. Although an equilibrium configuration was obtained for the numerical system after discrete crack insertion, the lack of consistency between stresses and strains undermined the numerical solution.

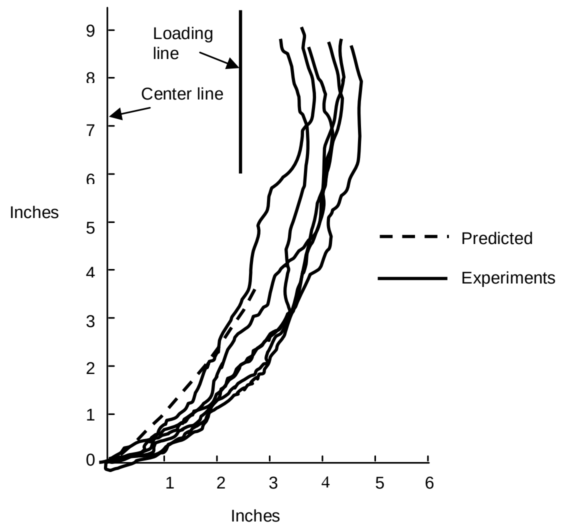

Figure 7: Comparison between the observed and predicted crack trajectories for mixed-mode analysis (adapted from [19]).

The last strategy showed more promising results in terms of discrete crack evolution. The approximations for the mapped variables improved in relation to that obtained in the previous strategies. These approximations were made at time t-Δt and the variables were updated at time t through the trial elastic strain increment. This allows the compatibility in the stress-strain fields and a more stable numerical solution after discrete crack insertion and propagation. The predicted crack trajectories match with the trajectories observed in the experiments, as shown in the example.

Nevertheless, the simulation of cohesive crack of arbitrary direction using discrete models is still an opened issue. Apparently, the mapping of history-dependent variables is a major drawback in this process, impeding the development of a general FEM code using the discrete approach. Although a good estimate of the crack trajectory is possible using the numerical model presented in this paper, it was not possible to represent the correct post-peak behavior of the structure, and investigations should be carried on this subject in the future. As a suggestion that can led to a better representation of the post-peak behavior of the structural system, the use of interface elements must be tested in the proposed model in order to control the residual forces that emerge after nodes separation due to discrete crack insertion.

References

[1] Hillerborg, A., Modéer, M. & Petersson, P.E., Analysis of crack formation and crack growth in concrete by means of fracture mechanics and finite elements. *Cement and Concrete Research*, **6**, pp. 773–782, 1976.

[2] Bazant, Z.P. & Planas, J., *Fracture and Size Effect in Concrete and Other Quasibrittle Materials*. CRC Press: Boca Raton-Florida - USA, 1998.

[3] Rots, J.G., *Computational modeling of concrete fracture*. Ph.D. thesis, Delft University of Technology, Delft - The Netherlands, 1988.

[4] Wawrzynek, P.A. & Ingraffea, A.R., Interactive finite element analysis of fracture processes: an integrated approach. *Theor Appl Fract Mech*, **8**, pp. 137–150, 1987.

[5] Bittencourt, T.N., Wawrzynek, P.A., Ingraffea, A.R. & Sousa, J.L., Quasi-automatic simulation of crack propagation for 2d lefm problems. *Engineering Fracture Mechanics*, **55(2)**, pp. 321–334, 1996.

[6] Potyondy, D., Wawrzynek, P. & Ingraffea, A.R., An algorithm to generate quadrilateral or triangular element surface meshes in arbitrary domains with applications to crack propagation. *International Journal for Numerical Methods in Engineering*, **38**, pp. 2677–2701, 1995.

[7] Wawrzynek, P.A., *Discrete modeling of crack propagation: theoretical aspects and implementation issues in two and three dimensions*. Ph.D. thesis, Cornell University, 1991.

[8] Bittencourt, T.N., Ingraffea, A.R. & Llorca, J., *Fracture Mechanics of Concrete Structures: Simulation of arbitrary cohesive crack propagation*. Elsevier Applied Science: London, 1992.

[9] Einsfeld, R.A., Elwi, A.E., Bittencourt, T.N. & Martha, L.F., Numerical simulation of fracturing in concrete structures using a combination of smeared and discrete approaches. *International Journal of Rock Mechanics and Mining Sciences*, **34(3-4)**, p. 552, 1997.

[10] Einsfeld, R.A. & Velasco, M.S.L., Fracture parameters for high-performance concrete. *Cement and Concrete Research*, **36(3)**, pp. 576–583, 2006.

[11] Erdogan, F. & Sih, G.C., On the crack extension in plates under plane loading and transverse shear. *Journal of Basic Engineering - ASCE*, **85**, pp. 519–527, 1963.

[12] Mantyla, M., *Introduction to solid modeling*. Computer Science Press: Rockville - MD, 1988.

[13] Einsfeld, R.A., Martha, L.F. & Bittencourt, T.N., Combination of smeared and discrete approaches with the use of interface elements. *European Congress on Computational Methods in Applied Sciences and Engineering (ECCOMAS 2000)*, Barcelona - Spain, p. 382, 2000.

[14] Lee, N.S. & Bathe, K.J., Error indicators and adaptive remeshing in large deformations finite element analysis. *Finite Elements in Analysis and Design*, **16**, pp. 99–139, 1994.

[15] Einsfeld, R.A., Roehl, D., Bittencourt, T.N. & Martha, L.F., Mapping of local variables due to remeshing in non-linear plasticity problems. *IACM - WCCM IV - Fourth World Congress on Computational Mechanics*, Buenos Aires - Argentina, p. I: 511, 1998.

[16] Manual, M.U., *L. F. Martha*. TeCGraf - PUC-Rio. (in Portuguese).

[17] Elwi, A.E., *FEPARCS 92 - A description and user's manual*. Department of Civil Engineering - University of Alberta, 1992.

[18] Pramono, E. & Willam, K., Fracture energy-based plasticity formulation of plain concrete. *Journal of Engineering Mechanics - ASCE*, **115(6)**, pp. 1183–1204, 1989.

[19] Arrea, M. & Ingraffea, A.R., Mixed-mode crack propagation in mortar and concrete. Technical report, Cornell University, Ithaca-New York - USA, 1982.

Brazilian Society of Mechanical Sciences and Engineering, ISBN 978-85-85769-30-7